Federal Aviation Administration

Report on Pilot Response Times from the March 2010 Human in the Loop Data Collection Effort

Flight Systems Laboratory
DOT-FAA-AFS-450-67

June 2011

Flight Systems Laboratory
6500 S. MacArthur Blvd.
Systems Training Building Annex, RM 217
Oklahoma City, Oklahoma 73169
Phone: (405) 954-8191

OK-11-3090

NOTICE

DOT-FAA-AFS-450-67

Flight Systems Laboratory
Flight Technologies and Procedures Division
Flight Standards Service

Report on Pilot Response Times from the March 2010 Human in the Loop Data Collection Effort

Reviewed by:

6/22/11

Harry Hodges **Date**
Manager, Flight Systems Laboratory, AFS-450

Released by:

6/22/11

Leslie H. Smith **Date**
Manager, Flight Technologies and Procedures Division, AFS-400

June 2011

Technical Report

Technical Report Documentation Page

1. Report No.	2. Government Accession No.	3. Recipient's Catalog No.
DOT-FAA-AFS-450-67		

4. Title and Subtitle
Report on Pilot Response Times from the March 2010 Human in the Loop Data Collection Effort

5. Report Date
June 2011

6. Author(s)
Greg Cox, AFS-450; Dr. James Yates, ISI; Jim Savage, ISI

7. Performing Organization Code
AFS-450

8. Performing Organization Name and Address
Federal Aviation Administration
Flight Systems Laboratory, AFS-450
6500 S MacArthur Blvd., STB Annex, RM 217
Oklahoma City, OK 73169

9. Type of Report and Period Covered
Technical Report

10. Sponsoring Agency Name and Address
Federal Aviation Administration
Flight Systems Laboratory, AFS-450
6500 S Mac Arthur Blvd., STB Annex, RM 217
Oklahoma City, OK 73169

11. Supplementary Notes

12. Abstract
In support of the Accelerating Next Generation Air Transportation System (NextGen) initiative, a Human in the Loop (HITL) data collection effort was accomplished to determine Pilot Response Time (PRT) to Air Traffic Controller breakout instructions during Simultaneous Parallel Independent Approaches to Closely Spaced Runways. Using a standard ASR-9 surveillance radar, and a Standard Automation Replacement System (STARS) Air Traffic Control workstation with Final Monitor Aid (FMA) display and alerting, the current runway separation standards are 4300 feet between runway centerlines and a No Transgression Zone (NTZ) width of 2000 feet. For this data collection effort (DCE), the runway spacing was reduced to 3000 feet and the NTZ width to 1200 feet. The resulting PRT Probability Distribution Function (pdf), and the aircraft dynamic pdf's, determined additionally, will be used as inputs to refine the Airspace Simulation and Analysis Tool (ASAT), a fast-time simulation to evaluate the level of risk of operations based on these runway spacing and NTZ dimensions.

13. Key Words
Simultaneous Parallel Independent Approaches
No Transgression Zone (NTZ)
Normal Operating Zone (NOZ)
Blunder
Deviation
Localizer
Instrument Landing System (ILS)
Human in the Loop (HITL)
Final Monitor Aid (FMA)
Airport Surveillance Radar (ASR)
Standard Automation Replacement System (STARS)

14. Distribution Statement
Controlled by AFS-450

15. Security Classification of This Report
Unclassified

16. Security Classification of This Page
Unclassified

EXECUTIVE SUMMARY

The Federal Aviation Administration (FAA) is identifying possible improvements to Closely Spaced Parallel Operations (CSPO) by evaluating closer runway spacing, one of the main parameters and a key capacity enabler, which affect airport capacity in less than visual conditions. The goal is to increase capacity during IMC operations and to maintain the current level of safety.

Other parameters affecting the operation include the navigation system used, radar surveillance capabilities, the air traffic automation system, runway threshold stagger and the risk of collision due to one aircraft unexpectedly blundering toward the aircraft on the parallel final approach course.

The purpose of this data collection effort was to determine the Pilot Response Time (PRT) to controller instructions to prevent a possible collision.

A Human in the Loop (HITL) data collection effort (DCE) was conducted in March 2010, using the FAA's Airbus A330 and Boeing B737 Level D flight simulators linked to two Air Traffic Control radar monitor controller workstations. Pilot response times were evaluated with pilots flying parallel ILS approaches and performing as they would in actual NAS operations. Monitor controllers used a Standard Terminal Automation Replacement System (STARS) Final Monitor Aid (FMA) with a color digital display, 4:1 aspect ratio, visual and aural alerts, and an Airport Surveillance Radar ASR-9 with a 4.8 second update rate.

A modified John F. Kennedy International Airport was chosen as the test airport, with 3000 ft separating the parallel runways with no threshold stagger. Due to the close proximities of aircraft in the July 2009 DCE (See Reference 3), Traffic Alert and Collision Avoidance System (TCAS) Resolution Advisories (RA) corrupted the data for determining pilot and controller response times. This follow-on PRT DCE was conducted with RAs inhibited. (Note – PRT starts when the final controller depresses the PTT)

The PRT mean for rolling the Airbus was 8.242 seconds for the Boeing the mean was 7.435 seconds. The PRT mean for throttle response for the Airbus was 9.061 seconds and for the Boeing the mean was 8.965 seconds.

To obtain the most accurate fast-time simulation results, it is recommended that the regression lines and residual probability density functions determined in this report be used in future simulations.

TABLE OF CONTENTS

LIST OF ILLUSTRATIONS

List of Tables

1.0. Introduction

The Federal Aviation Administration (FAA) Next Generation Air Transportation System (NextGen) Implementation Plan (NGIP) and the National Airspace System (NAS) Enterprise Architecture (EA) identify improvements to Closely Spaced Parallel Operations (CSPO) as a key future capacity enabler, with three high level goals:
Increasing Capacity: Reduce the impact of lower visibility conditions by closing the gap in capacity between Visual Meteorological Conditions (VMC) and Instrument Meteorological Conditions (IMC).

- Reducing Delays: Reduce system wide NAS delays.
- Maintaining Safety Standards: Ensure an acceptable level of safety exists in reduced visibility conditions with an increased number of approach operations to near that of VMC.

To meet these goals, the FAA is investigating methods to conduct closely spaced parallel independent approaches at runway spacing closer than currently authorized using a standard ASR-9 surveillance radar, and a STARS Air Traffic Control workstation with Final Monitor Aid display and alerting. Under these conditions, the current runway separation standards are 4300 feet between runway centerlines and a NTZ width of 2000 feet. For this data collection effort, the runway spacing was reduced to 3000 feet and the NTZ width to 1200 feet.

The distance between parallel runways is one of the main parameters that affects airport capacity and determines whether independent (higher throughput), dependent (lower throughput), or single runway arrival operations can be conducted. Other factors include the navigation system, an airport's radar surveillance capabilities, controller displays and runway threshold stagger. A principal safety concern is the risk of collision due to a blunder, where one aircraft unexpectedly turns toward the aircraft on the other parallel final approach course, putting the aircraft on the parallel final at risk.

A test of these parameters was conducted in March 2010, using the FAA's Boeing B737-800 and Airbus A330-200 Level D flight simulators linked to the two Air Traffic Control radar monitor controller workstations located within the Flight Operations Simulation Laboratory at the Mike Monroney Aeronautical Center, in Oklahoma City.

The John F. Kennedy International Airport was chosen as the test location due to its runway geometry. Runway 22R was modified to duplicate Runway 22L in all aspects and moved so that the runway centerlines were separated by 3000 feet with no threshold stagger. The NTZ, centered between the runways, was reduced to 1200 feet, leaving an NOZ of 900 feet between each runway centerline and the respective edge of the NTZ.

The purpose of this data collection effort was to satisfy Phase 1 of the Safety Risk Management Panel's Project Plan CSPO-001, "Simultaneous Independent Dual Straight-In ILS Approaches with Runway Centerlines at 3,000 Feet, using a 4.8 Second Surveillance Update Rate" (reference 1). This was a Human in the Loop test with both pilots and controllers performing as they would in actual NAS operations. The monitor controllers used the STARS FMA display, a color digital display with 4:1 aspect ratio, providing visual and aural alerts.

The TCAS is an airborne system developed by the FAA that operates independently from the ground-based Air Traffic Control system. TCAS was designed to increase cockpit awareness of proximate aircraft and to serve as a "last line of defense" for the prevention of mid-air collisions. TCAS provides TAs, indications to the flight crew that a particular intruder is a potential threat, and RAs, indications that recommend a maneuver to provide separation from the threat.

Due to the close proximities of the simulated aircraft during the configuration utilized in the July 2009 DCE (See Reference 3), TCAS RAs were issued just before controller instructions for a breakout maneuver. Unfortunately, pilot responses to these nuisance RAs corrupted the data for determining pilot and controller response times. This follow-on, Pilot Response Time DCE, was conducted with RAs inhibited to determine pilot response times. Also, further air traffic controller HITL DCEs were conducted with only controller participants to determine controller response times. The resultant data will be contained in another technical report.

1.1. Background

In support of NextGen initiatives, a HITL DCE was accomplished to determine pilot and controller response times for simultaneous parallel independent approaches to closely spaced runways. At the direction of the Accelerating NextGen Committee, the data collection effort evaluated runway spacing and NTZ dimensions that were significantly reduced from the current standards using an ASR-9 airport surveillance radar and STARS with FMA display. Those standards are 4300 feet between runway centerlines and an NTZ width of 2000 feet. For this data collection effort, the spacing was reduced to 3000 feet and 1200 feet respectively, as shown in the figure below.

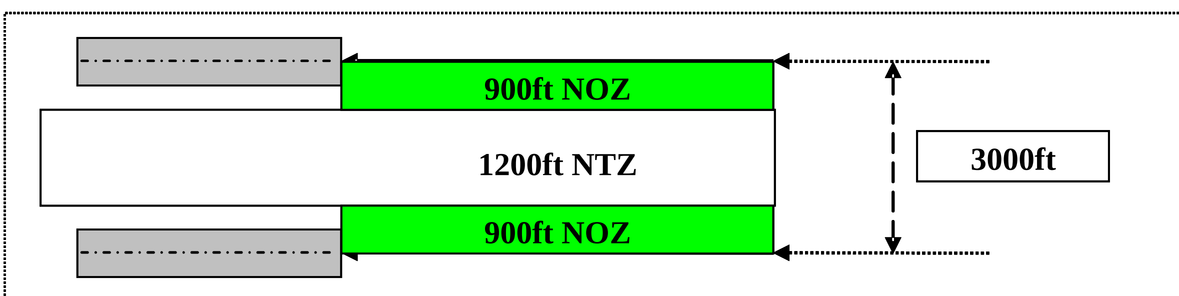

Figure 1: Runway Spacing and NTZ/NOZ Depictions

2.0. Discussion

The airport chosen for this simulation effort was John F. Kennedy International, using runways 22L and 22R. Runway 22R was modified to match 22L by moving its threshold in order to remove the stagger, and adding the identical approach light array configuration. Finally, Runway 22R was moved so that the runway centerline spacing was 3000 feet, as shown in Figure 1. The DCE was conducted in March 2010, using the FAA's Boeing B737-800 and Airbus A330-200 Level D flight simulators linked to the two Air Traffic Control radar monitor controller workstations located in the Flight Operations Simulation Laboratory.

2.1. Objectives

The objectives of the test were to:

- Perform real-time data collection focused on pilot response times while conducting dual simultaneous independent parallel instrument approaches using a runway spacing of 3000 feet, no threshold stagger, ASR-9 surveillance radar with update rate of 4.8 seconds and STARS with FMA display.
- Determine pilot response times during "at-risk" blunder scenarios to include a mix of responding and non-responding blundering aircraft using 20 and 30 degree angles of blunder. Blunders were simulated using computer generated aircraft (pseudo aircraft) operated by trained specialists. An at-risk blunder was a blunder in which the two aircraft were aligned in such a way that if the monitor controller and/or the endangered pilot did not react in a timely manner, the pseudo-aircraft and the flight simulator would pass within 500 feet Center of Gravity (CG) to CG causing a Test Criteria Violation (TCV).
- Determine pilot response times during a missed approach breakout caused by an NTZ penetration by the opposite parallel aircraft. No blunders were simulated during the missed approach maneuver. Instead, the pseudo aircraft deviated slightly towards the NTZ (10 to 15 degrees) during a simultaneous missed approach or balked landing.
- Collect the specified aircraft operational/aerodynamic data for the A330-200 and B737-800 during approach and missed approach breakouts.

3.0. Data Analysis

Software was developed for a computer system that is capable of operating two simulated radar displays and presenting coordinated pseudo aircraft tracks with flight simulator tracks on simulated ASR-9 surveillance radar with an update rate of 4.8 seconds and STARS with FMA display. Pilot response time was measured from the start of the controller instruction, i.e., at the instant the controller pressed the Push To Talk (PTT) switch, until the pilot made an input to either the roll or throttle control. Note that the time required for the controller to deliver the complete message is another variable that was implicitly included in the pilot response time. Other data of interest were pilot induced aircraft parameters such as maximum bank angle, roll rate, roll acceleration, throttle time, climb rate and climb acceleration.

3.1. Data Collection

The variables either recorded by the system or derived from recorded variables included the following:

1. Monitor controller breakout instruction start time from time of warning or alert
2. Pilot roll time
3. Pilot pitch time
4. Pilot throttle time
5. Pilot autopilot disconnect time
6. Maximum roll angle
7. Roll rate, degrees per second
8. Roll acceleration, degrees per second per second
9. Monitor controller breakout instruction start to pilot roll time
10. Monitor controller breakout instruction start to pilot pitch time
11. Monitor controller breakout instruction start to pilot throttle time

Other variables that were derived from pilot and controller questionnaires:

1. Pilot qualified for line operations? (yes or no)
2. First officer qualified for line operations? (yes or no)

3.2. Statistical Analysis

One important purpose of the simulation was to collect data that can be used to develop probability density functions (pdf). A pdf is a function that describes the relative likelihood for a random variable to occur at a given point. The pdfs can be used in a fast-time, Monte Carlo computer simulation to determine the probability of a collision during closely spaced parallel approach operations due to a blunder. The probability of a collision can be compared to a standard probability or risk, i.e., a target level of safety, to determine the acceptability of the operation. A mathematical algorithm is used to determine a pdf of best fit to the data in question such as pilot response time. Confidence in the suitability of the derived pdf increases with increased numbers of observations in the data set.

In this simulation, the data of interest were pilot response times and the resultant aircraft dynamics. Analysis of the questionnaire data revealed that all the pilots were qualified and current in the two aircraft used in the simulation. Therefore, it was not necessary to determine whether there could be differences in the response times of qualified versus unqualified pilots. However, the test involved aircraft constructed by two different manufacturers using different control systems and even different cockpit controls such as the side stick for the Airbus and the conventional control yoke for the Boeing. These differences could result in different distributions of response times for the two aircraft. In addition, the two different aircraft most likely have different capabilities affecting roll and/or climb rates.

Statistical tests have been devised to enable the analyst to decide whether two or more independent samples should be regarded as having come from the same population. Values from different independent samples almost always differ somewhat in means, variance, and other measures that describe properties of the data. The problem is to determine whether the observed sample differences signify differences among populations or whether they are merely the chance variations that are to be expected among random samples from the same population.

One of the most powerful and flexible statistical tests of differences in means of independent sample sets is analysis of variance (ANOVA). ANOVA is a parametric test that is based on certain assumptions about the data, and assumes that the data was generated from normal distributions, but having the same variance. These conditions are not often completely met in practical applications and it will be shown that the curves that best fit the data sets are bounded and not from a normal distribution. However, much study has been done by statisticians to ascertain the effects of violations of the assumptions. In most cases, violations of the assumptions, even fairly extreme ones, do not severely affect the outcome of the analysis of variance. ANOVA is easily performed using any statistical package and, in the case of Statistical Package for the Social Studies (SPSS), Levene's test (reference 2), a test of homogeneity of variance, is conducted concurrently with ANOVA. Levene's test is useful since it provides another measure of whether the data sets are similar enough to be pooled into one set.

The objective of many scientific investigations is to understand and explain the relationships among variables. Frequently, one wants to know how and to what extent a certain response variable is related or influenced by another variable. In the current study, it seems reasonable that the maximum bank angle could be influenced or related to the roll rate, i.e., a rapid roll rate might lead to a large bank angle. In most cases, the relationships are not known and are too complicated to be described by a related variable. In this case, one variable, say maximum bank angle, is treated as a random variable that varies around a mean or average value which depends on the value of the predictor variable such as roll rate. Repeated trials with identical roll rate values would not have the same maximum bank angle each time, but would form a distribution of values about a predicted maximum bank angle.

The first thing that must be done when considering possible relationships between variables is to determine if there is a relationship and the extent of the relationship. This is usually done using some measure of correlation such as the Spearman rank correlation coefficient. This statistic, sometimes called rho, is a non-parametric measure of correlation. Non-parametric is defined as not requiring any assumptions about the nature of the variables being tested, such as normality.

If the Spearman test indicates that there is a correlation then some method of relating the two variables must be devised. The simplest method is to assume that a linear relationship exists, choose one variable to be the independent variable, and then perform a linear regression to obtain a best-fit straight line. A linear regression of a data set that consists of two variables X and Y is a least squares line through the two dimensional data. Because of sampling variation the observed values or points will not all lie on the line, but will be scattered to some degree about the line. The regression line equation will have the form:

$$Y = \beta_0 + \beta_1 X$$

Suppose that X_i is a value of X from the data and Y_i is its corresponding Y value. An estimated value of $\hat{Y}_i$ can be derived from the equation of the regression line by substituting X_i into the equation. The difference between the Y values, $\overline{Y}_i = Y_i - \hat{Y}_i$, is called a residual. The set of residuals forms a distribution of data with mean zero and a probability density curve can be fitted to the set. Sampling in a Monte Carlo simulation is done by first computing a value of X from the pdf for the X data, then computing the predicted value of Y, $\hat{Y}$, from the regression equation, and then computing a value of the residual, $\overline{Y}$, from the residual pdf. The value of Y associated with the value of X is computed by the equation:

$$Y = \overline{Y} + \hat{Y}$$

Ideally, the set of residuals will be normally distributed. If the set of residuals is not normally distributed then the residuals can be fitted with a curve such as a Johnson curve.

3.3 Fitting Johnson Probability Density Functions

The Johnson family of empirical distributions is based on transformations of a standard normal variate. An advantage of such a transformation is that estimates of the percentiles of the fitted distribution can be obtained either from a table of areas under a standard normal distribution or from a computer program which computes areas under a standard normal distribution. Another advantage is during a Monte Carlo simulation variates from the distribution are readily computed from the standard normal distribution. The Johnson distributions are divided into three families as follows:

1. The S_L family is characterized by the transformation:

$$z = \gamma + \delta \ln\left(\frac{x - \varepsilon}{\lambda}\right), \; x > \varepsilon,$$

where *x* is the variable to be fitted by the Johnson distribution and *z* is a standard normal variate. Each curve in this family is bounded on the left by ε and is unbounded on the right.

2. The S_B family is characterized by the transformation:

$$z = \gamma + \delta \ln\left(\frac{x-\varepsilon}{\lambda+\varepsilon-x}\right),\ \varepsilon < x < \varepsilon + \lambda.$$

where *x* is the variable to be fitted by the Johnson distribution and *z* is a standard normal variate. Each curve in this family is bounded on the left by ε and on the right by ε + λ.

3. The S_U family is characterized by the transformation:

$$z = \gamma + \delta \sinh^{-1}\left(\frac{x-\varepsilon}{\lambda}\right),\ -\infty < x < \infty.$$

where *x* is the variable to be fitted by the Johnson distribution and *z* is a standard normal variate. Each curve in this family is unbounded and unimodal.

4.0 Comparison of Roll and Throttle Response Times by Aircraft Type

Pilot response times were determined by pilot input to aileron and throttle controls. The roll response time data and throttle response time data were divided into two groups by aircraft type; Airbus and Boeing. Descriptive statistics, Levene's test of homogeneity of variances, and ANOVA test of means were run. Probability density functions were developed for each distinct data set.

4.1 Comparison of Roll Response Times by Aircraft Type

Tables 1, 2, and 3 indicate the standard statistics, results of the Levene's test and results of the ANOVA. Table 1 contains the descriptive statistics of roll response time. Table 2 indicates the results of Levene's test of homogeneity of variances. The table indicates that for the roll response time data, the probability of a Levene statistic being greater than 0.685 is 0.409. If the probability had been 0.05 or less, then a significant difference in variances would have been indicated and the data could not be pooled. However, table 3 indicates that for the roll response time data the probability of an F statistic being greater than 6.323 is only 0.013. Therefore, the means of the two roll response time data sets are significantly different and the Airbus and Boeing roll response time data sets cannot be combined into one set.

Table 1: Descriptive Statistics of Roll Response Time

Descriptive Statistics

Roll Response Time

					95% Confidence Interval for Mean			
	N	Mean	Std. Deviation	Std. Error	Lower Bound	Upper Bound	Minimum	Maximum
Airbus	68	8.242	2.1624	.2622	7.718	8.765	5.3	15.3
Boeing	90	7.435	1.8607	.1961	7.046	7.825	4.5	14.6
Total	158	7.782	2.0294	.1615	7.463	8.101	4.5	15.3

Table 2: Levene's Test of Homogeneity of Variances of Roll Response Time

Test of Homogeneity of Variances

Roll Response Time

Levene Statistic	df1	df2	Sig.
.685	1	156	.409

Table 3: ANOVA of Roll Response Time

ANOVA

Roll Response Time

	Sum of Squares	df	Mean Square	F	Sig.
Between Groups	25.188	1	25.188	6.323	.013
Within Groups	621.418	156	3.983		
Total	646.606	157			

4.2 Johnson PDF Curves for Roll Response Times by Aircraft Type

Figures 2 and 3 are graphs of the Johnson pdf curves that were fitted to the roll response time data. Included in the figures are histograms of the data sets. The values of the parameters are included in Appendix A. Goodness-of-fit tests indicated the curves fit the data very well. Results of goodness-of-fit tests are included in the tables.

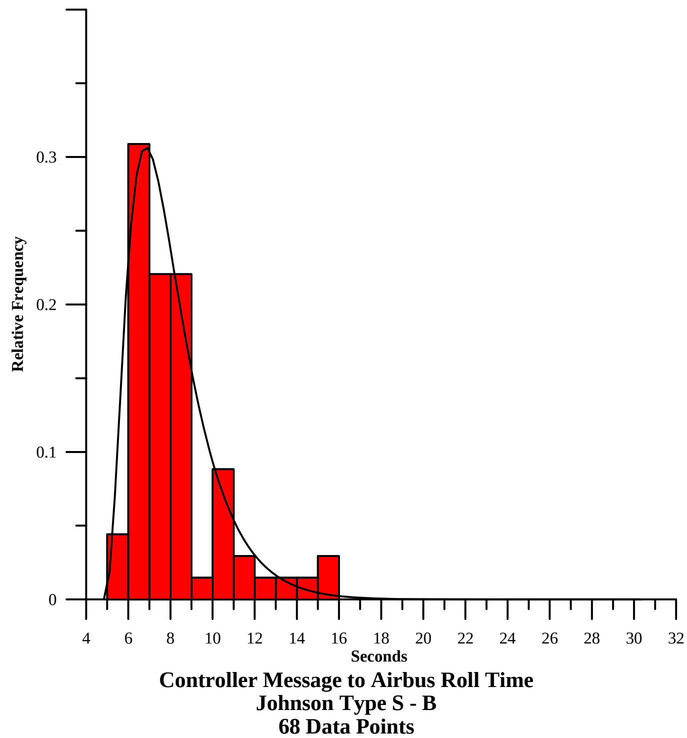

Figure 2: Johnson Curve fitted to Airbus Roll Response Time Data

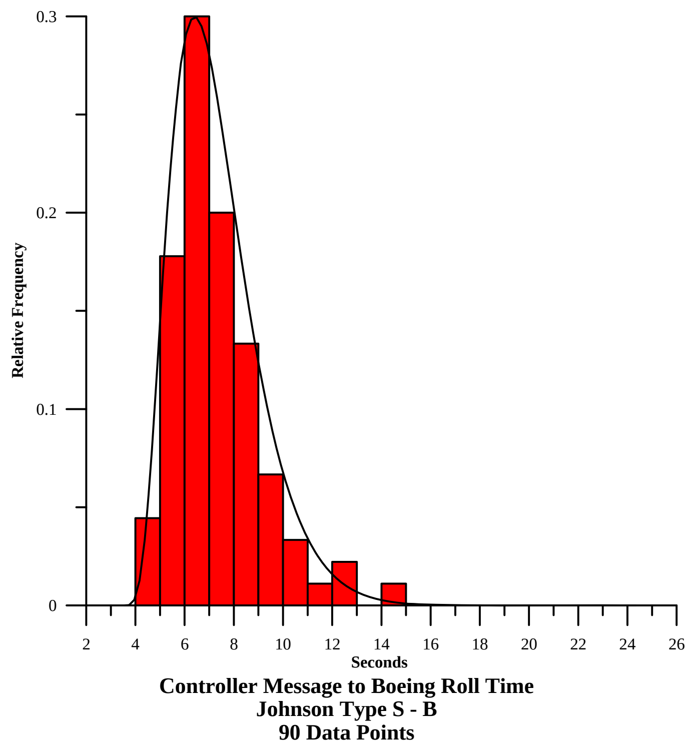

Figure 3: Johnson Curve fitted to Boeing Roll Response Time Data

4.3 Comparison of Throttle Response Times by Aircraft Type

Tables 4, 5, and 6 indicate the standard statistics, results of the Levene's test and results of the ANOVA. Table 4 contains the descriptive statistics of throttle response time. Table 5 indicates the results of Levene's test of homogeneity of variances. The table indicates that for the throttle response time data the probability of a Levene statistic being greater than 5.124 is 0.025. Since the probability is less than 0.05, a significant difference in variances is indicated and the data could not be pooled. However, table 6 indicates that for the throttle response time data, the probability of an F statistic being greater than 0.045, is 0.832. Therefore, the means of the two throttle response time data sets are not significantly different.

Table 4: Descriptive Statistics of Throttle Response Time

Descriptive Statistics

Throttle Response Time

	N	Mean	Std. Deviation	Std. Error	95% Confidence Interval for Mean		Minimum	Maximum
					Lower Bound	Upper Bound		
Airbus	66	9.061	3.2793	.4037	8.254	9.867	4.8	20.5
Boeing	93	8.965	2.4030	.2492	8.470	9.460	5.0	16.2
Total	159	9.005	2.7908	.2213	8.568	9.442	4.8	20.5

Table 5: Levene's Test of Homogeneity of Variances of Throttle Response Time

Test of Homogeneity of Variances

Throttle Response Time

Levene Statistic	df1	df2	Sig.
5.124	1	157	.025

Table 6: ANOVA of Throttle Response Time

ANOVA

Throttle Response Time

	Sum of Squares	df	Mean Square	F	Sig.
Between Groups	.352	1	.352	.045	.832
Within Groups	1230.227	157	7.836		
Total	1230.579	158			

4.4 Johnson PDF Curves for Throttle Response Times by Aircraft Type

Figures 4 and 5 are graphs of the Johnson pdf curves that were fitted to the throttle response time data. Included in the figures are histograms of the data sets. The values of the parameters are included in Appendix A. Goodness-of-fit tests indicated the curves fit the data very well. Results of goodness-of-fit tests are included in the tables.

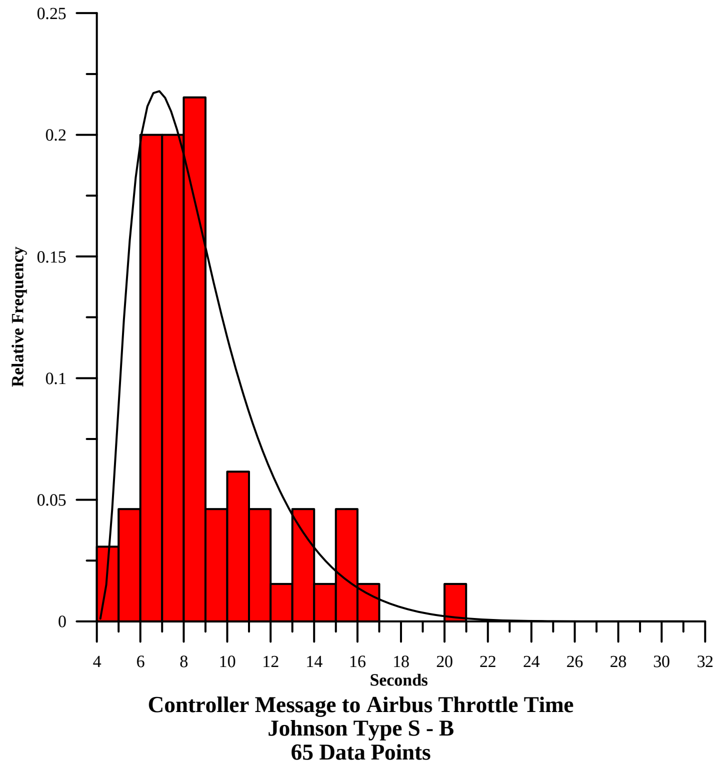

Figure 4: Johnson Curve fitted to Airbus Throttle Response Time Data

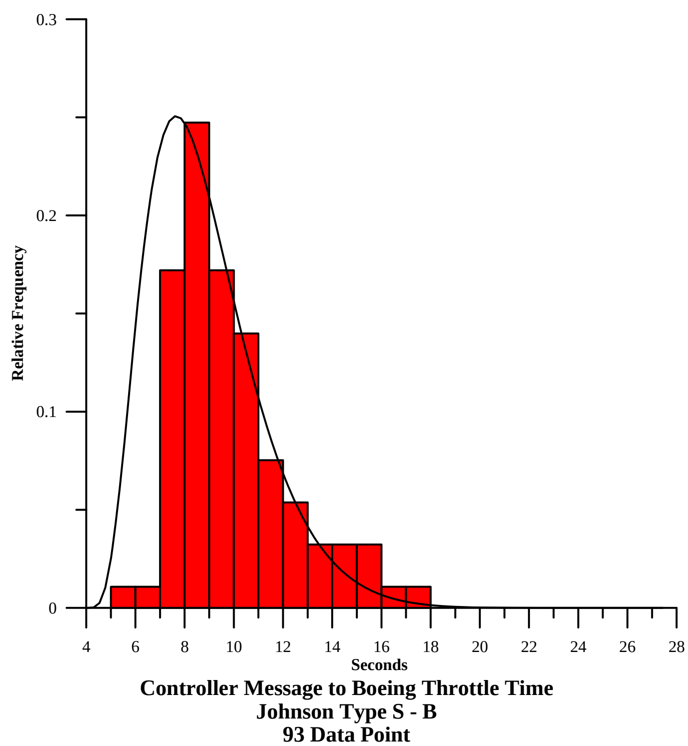

Figure 5: Johnson Curve fitted to Boeing Throttle Response Time Data

4.5 Correlation of Roll Response Time with Throttle Response Time

After pilot response time curves for roll and throttle response have been developed, then the next question is how these should be utilized in the simulation. For each type of aircraft is the roll time independent of the throttle time or is there an association? A possible association is that one of the times is more likely to be first, i.e., perhaps pilots tend to begin the climb before the roll. Another possibility to consider is that a pilot who has a delayed response to initiate a climb may also delay the start of a roll, i.e., the two reaction times tend to be close to one another. There are various ways to check for some kind of correlation or association between variables. Two simple methods involve a visual inspection of scatter plots of the two variables and tests of correlation like the Spearman rho test. The Spearman rho test is a test for a linear association. It tests for an association like that of a pilot who takes a longer time to start the climb also takes a longer time to start the roll. Figures 6 and 7 are scatter plots of roll versus throttle time for the two types of aircraft. The scatter plots indicate there is possibly a slight positive linear association. Tables 7 and 8 display the results of the Spearman rho test for the Airbus and Boeing data sets.

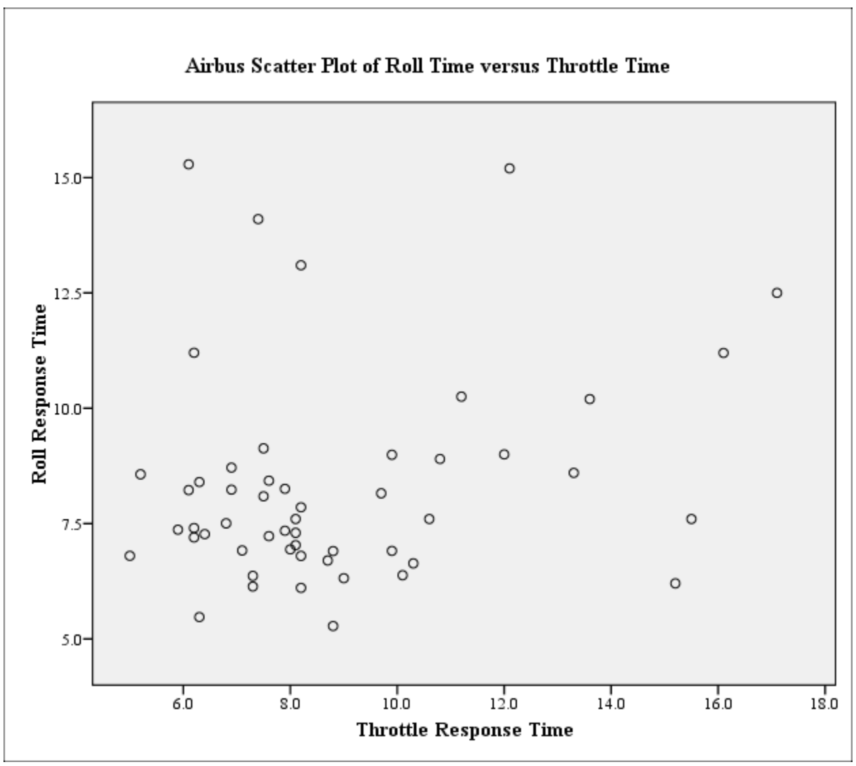

Figure 6: Airbus Scatter Plot of Roll Time versus Throttle Time

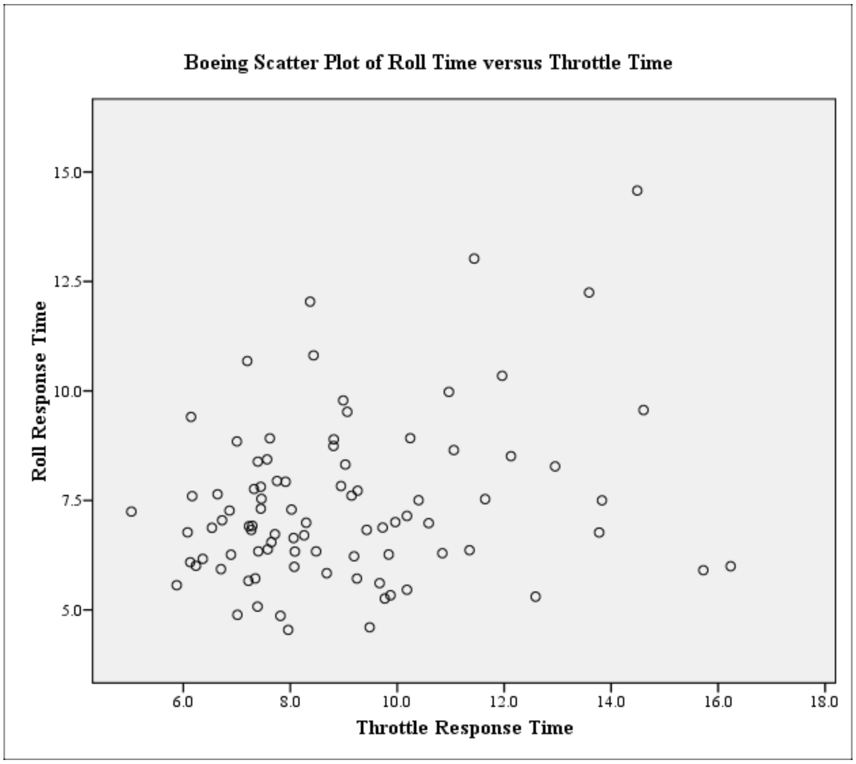

Figure 7: Boeing Scatter Plot of Roll Time versus Throttle Time

Table 7: Spearman's rho Test of Airbus Correlation of Roll Time versus Throttle Time

Airbus Correlations

			Roll Response Time	Throttle Response Time
Spearman's rho	Roll Response Time	Correlation Coefficient	1.000	.087
		Sig. (2-tailed)	.	.538
		N	68	52
	Throttle Response Time	Correlation Coefficient	.087	1.000
		Sig. (2-tailed)	.538	.
		N	52	66

Table 8: Spearman's rho Test of Boeing Correlation of Roll Time versus Throttle Time

Boeing Correlations

			Roll Response Time	Throttle Response Time
Spearman's rho	Roll Response Time	Correlation Coefficient	1.000	.155
		Sig. (2-tailed)	.	.150
		N	90	88
	Throttle Response Time	Correlation Coefficient	.155	1.000
		Sig. (2-tailed)	.150	.
		N	88	93

The two tables are matrices that indicate the value of Spearman's rho and the probability of getting a rho value of that size if there is no linear correlation. The value of rho in Table 7 is 0.087, with a probability of 0.538. Therefore, we cannot discard the hypothesis that there is no linear relationship between the two variables, roll time and throttle time, for the Airbus data. In table 8 the value of rho is 0.155, with a probability of 0.150. Therefore, we cannot discard the hypothesis that there is no linear relationship between the two variables, roll time and throttle time, for the Boeing. This means that during the Monte Carlo simulation the roll time and throttle time for a particular run can be determined independently from the appropriate probability distributions.

5.0 Comparison of Flight Dynamics by Aircraft Type

Other variables besides pilot reaction times are needed to simulate the breakout path of the evading airplane. Four variables, maximum bank angle, roll rate, climb rate, and climb acceleration are used. It is desirable that the Airbus maximum bank angle data be combined with the Boeing maximum bank angle data to achieve a larger data set for fitting a probability density curve, however; there is the possibility that the data sets are statistically different and cannot be combined. The same statement is true for the other three variables used in the caparison. Therefore, the data sets for each variable were tested by aircraft type to determine whether the sets could be combined.

5.1 Comparison of Rate of Climb Data by Aircraft Type

Tables 9, 10 and 11 display the comparative results for the rate of climb of the two aircraft. Table 10 indicates no significant difference in the dispersions or standard deviations of the two data sets. Table 11 indicates a significant difference in the means of the two data sets. Therefore, the two data sets cannot be combined into one set and two probability density functions are required. Figures 8 and 9 display histograms and probability density functions for the two data sets.

Table 9: Descriptive Statistics of Rate of Climb by Aircraft Type

Descriptive Statistics of Rate of Climb

ROC > 0 [FPM]

	N	Mean	Std. Deviation	Std. Error	95% Confidence Interval for Mean		Minimum	Maximum
					Lower Bound	Upper Bound		
Airbus	59	2222.458	655.57135571	85.34812	2051.615607	2393.301258	937.90150	3440.013
Boeing	84	1975.688	670.69601975	73.17894	1830.137918	2121.237835	764.89703	3861.581
Total	143	2077.502	673.30128167	56.30428	1966.199379	2188.805225	764.89703	3861.581

Table 10: Levene's Test of Homogeneity of Variances of Rate of Climb

Test of Homogeneity of Variances

ROC > 0 [FPM]

Levene Statistic	df1	df2	Sig.
.472	1	141	.493

Table 11: ANOVA of Rate of Climb

ANOVA of Rate of Climb

ROC > 0 [FPM]

	Sum of Squares	df	Mean Square	F	Sig.
Between Groups	2110483	1	2110483.392	4.779	.030
Within Groups	62263032	141	441581.788		
Total	64373515	142			

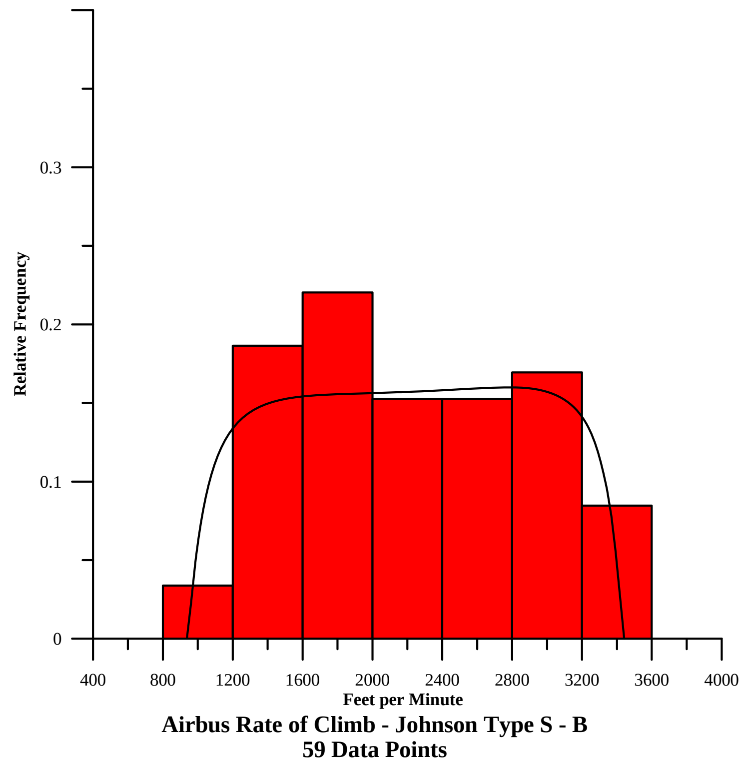

Figure 8: Airbus Rate of Climb

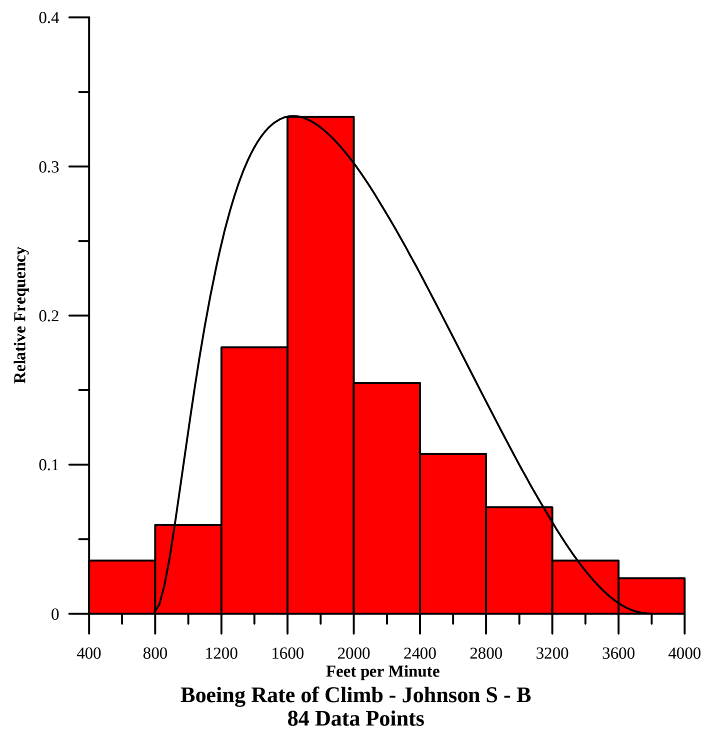

Figure 9: Boeing Rate of Climb

5.2 Comparison of Climb Acceleration Data by Aircraft Type

Tables 12, 13 and 14 display the comparative results for climb acceleration of the two aircraft. Table 13 indicates significant difference in the dispersions or standard deviations of the two data sets. Table 14 indicates a significant difference in the means of the two data sets. Therefore, the two data sets cannot be combined into one set and will require two probability density functions. Figures 10 and 11 display histograms and probability density functions for the two data sets.

Table 12: Descriptive Statistics of Climb Acceleration

Descriptive Statistics of Climb Acceleration

ROC Rate >0 [FPM/SEC]

	N	Mean	Std. Deviation	Std. Error	95% Confidence Interval for Mean		Minimum	Maximum
					Lower Bound	Upper Bound		
Airbus	59	279.9227	105.10961726	13.68411	252.5309410	307.3143719	107.73298	578.09331
Boeing	84	334.0389	135.39783586	14.77312	304.6557566	363.4220199	121.56863	698.03922
Total	143	311.7112	126.26503000	10.55881	290.8384360	332.5839883	107.73298	698.03922

Table 13: Levene's Test of Homogeneity of Variances of Climb Acceleration

ANOVA

ROC Rate >0 [FPM/SEC]

	Sum of Squares	df	Mean Square	F	Sig.
Between Groups	101496.3	1	101496.334	6.618	.011
Within Groups	2162389	141	15336.096		
Total	2263886	142			

Table 14: ANOVA of Climb Acceleration

ANOVA

ROC Rate >0 [FPM/SEC]

	Sum of Squares	df	Mean Square	F	Sig.
Between Groups	101496.3	1	101496.334	6.618	.011
Within Groups	2162389	141	15336.096		
Total	2263886	142			

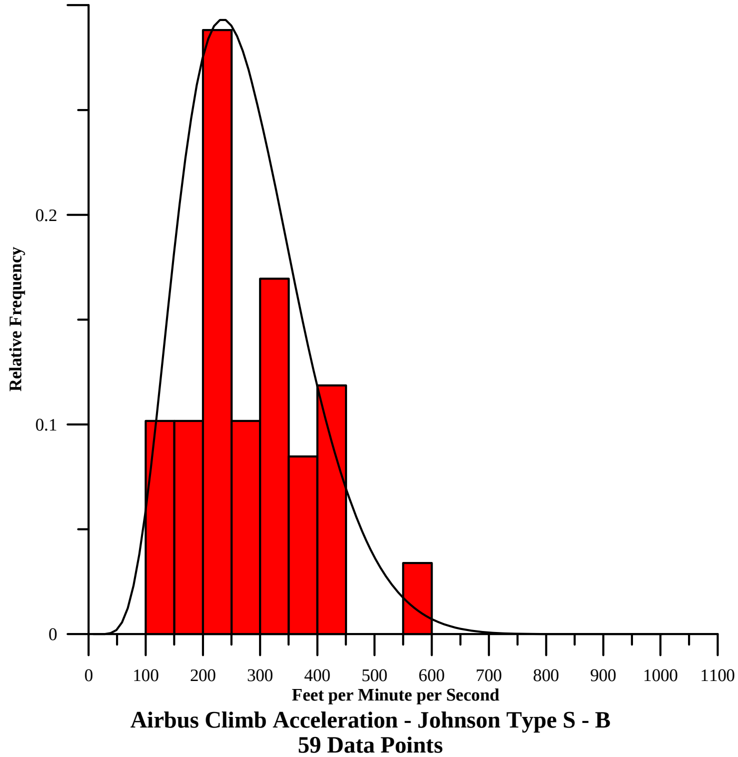

Figure 10: Airbus Climb Acceleration

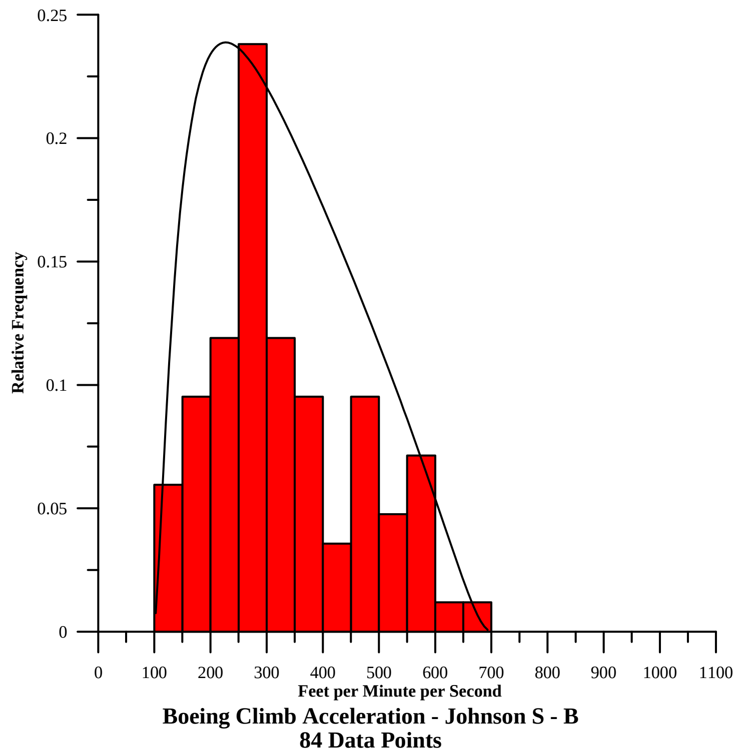

Figure 11: Boeing Climb Acceleration

5.3 Correlation of Climb Rate with Climb Acceleration

Tables 15 and 16 display the results of the Spearman rho test for the Airbus and Boeing rate of climb versus climb acceleration. The results indicate that there is a linear correlation for both aircraft data sets. Tables 17 and 18 display the results of the regression analysis. Figures 12 and 13 are scatter plots of the data for the Airbus and Boeing aircraft respectively.

Table 15: Spearman's rho Test of Airbus Correlation of Climb Rate versus Climb Acceleration

Airbus Correlations

			ROC > 0 [FPM]	ROC Rate >0 [FPM/SEC]
Spearman's rho	ROC > 0 [FPM]	Correlation Coefficient	1.000	.359**
		Sig. (2-tailed)	.	.006
		N	58	58
	ROC Rate >0 [FPM/SEC]	Correlation Coefficient	.359**	1.000
		Sig. (2-tailed)	.006	.
		N	58	58

**. Correlation is significant at the 0.01 level (2-tailed).

Table 16: Spearman's rho Test of Boeing Correlation of Climb Rate versus Climb Acceleration

Boeing Correlations

			ROC > 0 [FPM]	ROC Rate >0 [FPM/SEC]
Spearman's rho	ROC > 0 [FPM]	Correlation Coefficient	1.000	.555**
		Sig. (2-tailed)	.	.000
		N	84	84
	ROC Rate >0 [FPM/SEC]	Correlation Coefficient	.555**	1.000
		Sig. (2-tailed)	.000	.
		N	84	84

**. Correlation is significant at the 0.01 level (2-tailed).

Table 17: Airbus Regression Coefficients of Climb Rate versus Climb Acceleration

Airbus Coefficients ROC Independent, ROC Rate Dependent[a]

Model		Unstandardized Coefficients		Standardized Coefficients	t	Sig.
		B	Std. Error	Beta		
1	(Constant)	151.110	45.849		3.296	.002
	ROC > 0 [FPM]	.058	.020	.361	2.927	.005

a. Dependent Variable: ROC Rate >0 [FPM/SEC]

Table 18: Boeing Regression Coefficients of Climb Rate versus Climb Acceleration

Boeing Coefficients ROC Independent, ROC Rate Dependent[a]

Model		Unstandardized Coefficients		Standardized Coefficients	t	Sig.
		B	Std. Error	Beta		
1	(Constant)	121.306	39.321		3.085	.003
	ROC > 0 [FPM]	.108	.019	.533	5.710	.000

a. Dependent Variable: ROC Rate >0 [FPM/SEC]

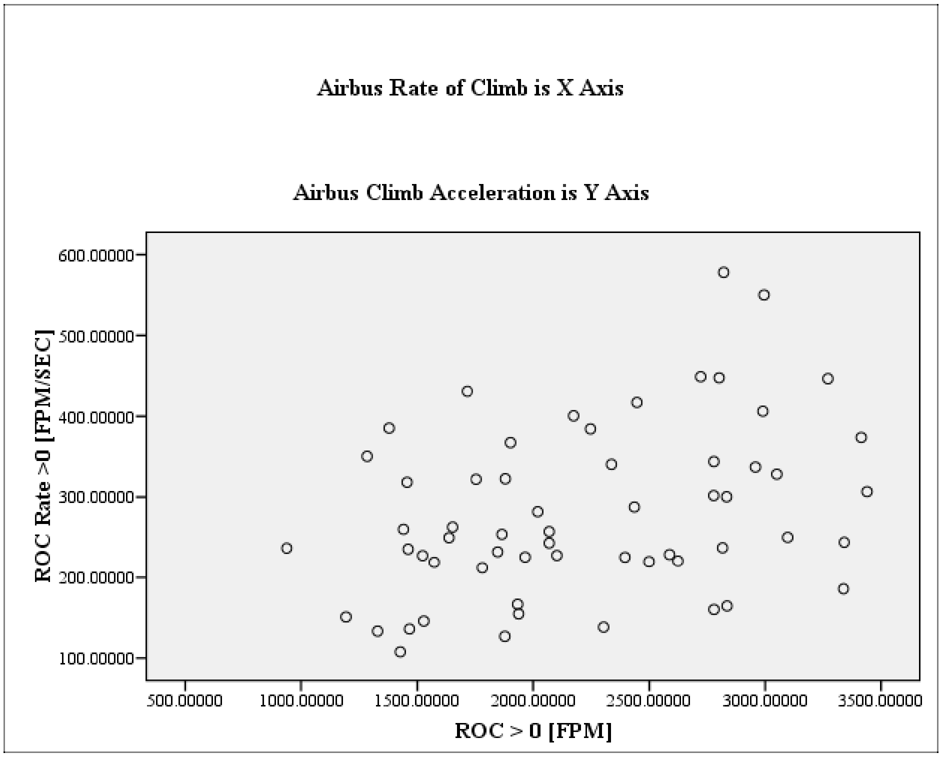

Figure 12: Airbus Scatter Plot of Climb Rate versus Climb Acceleration

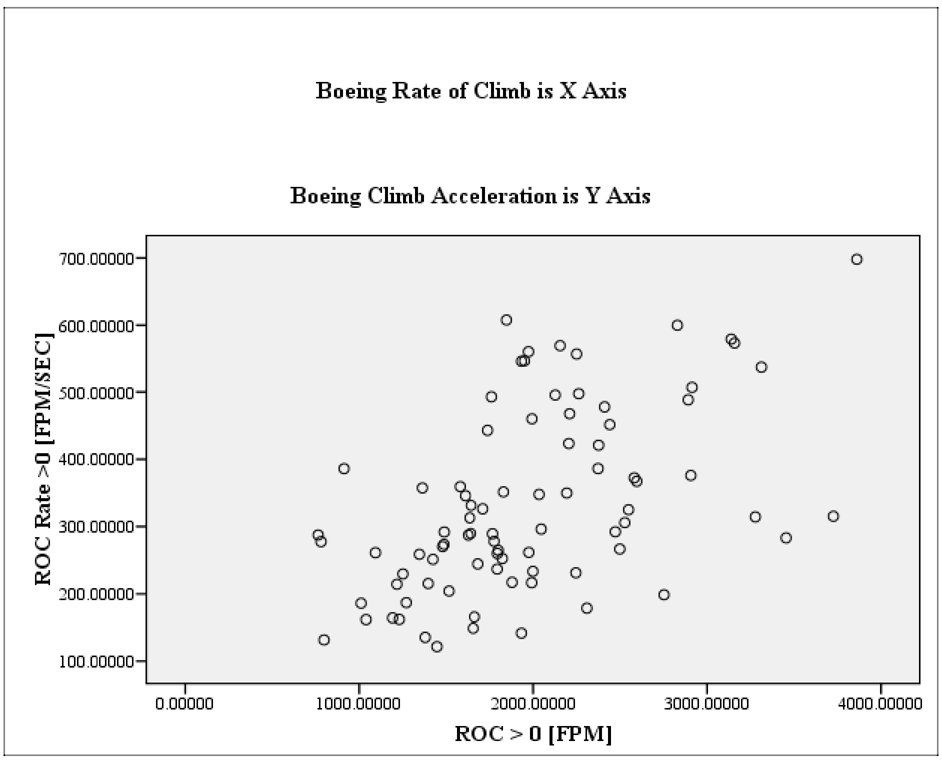

Figure 13: Boeing Scatter Plot of Climb Rate versus Climb Acceleration

5.4 Johnson Curves for the Sets of Climb Regression Residuals

Tables 19 and 20 display the results of two tests of normality, Kolmogorov-Smirnov and Shapiro-Wilk. In Table 19 the Kolmogorov-Smirnov test of Airbus residual data has a significance, or probability, of at least 0.200 and the Shapiro-Wilk test of Airbus residual data has a significance of 0.129. If either of these tests had produced a significance value less than 0.05, then the conclusion would have been that the data was not produced by a normal distribution. Therefore, the Airbus residual data can be modeled by a normal probability density function. The results of fitting a normal curve to the Airbus climb residual data are displayed in Figure 14. A Johnson S – B curve was also fitted to the data and is displayed in Figure 14. The Johnson curve closely follows the normal and has the advantage of being a bounded curve. Since a normal curve has infinite tails it is possible to draw very large or small unrealistic values while sampling in a Monte Carlo simulation. Since the Johnson curve is bounded, no unrealistic values can be drawn.

In Table 20 the Kolmogorov-Smirnov test of Airbus residual data has a significance, or probability, of at least 0.200 and the Shapiro-Wilk test of Boeing residual data has a significance of 0.292. Therefore, the Boeing residual data can be modeled by a normal probability density function. The results of fitting a normal curve to the Boeing climb residual data are displayed in Figure 15. A Johnson S – B curve was also fitted to the data and is displayed in Figure 15.

Table 19: Airbus Tests of Residual Normality for Climb Rate versus Climb Acceleration

Tests of Normality Airbus ROC Residuals

	Kolmogorov-Smirnov[a]			Shapiro-Wilk		
	Statistic	df	Sig.	Statistic	df	Sig.
Unstandardized Residual	.085	59	.200*	.968	59	.129

*. This is a lower bound of the true significance.

a. Lilliefors Significance Correction

Table 20: Boeing Tests of Residual Normality for Climb Rate versus Climb Acceleration

Tests of Normality Boeing ROC Residuals

	Kolmogorov-Smirnov[a]			Shapiro-Wilk		
	Statistic	df	Sig.	Statistic	df	Sig.
Unstandardized Residual	.085	84	.200	.982	84	.292

a. Lilliefors Significance Correction

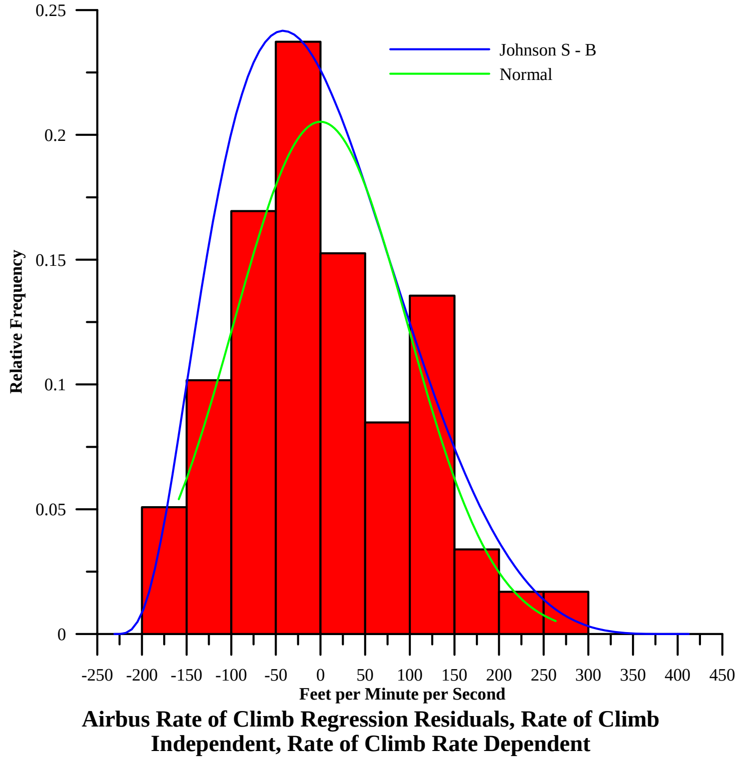

Figure 14: Normal Curve and Johnson S – B Curve Fitted to Airbus Climb Residual Data

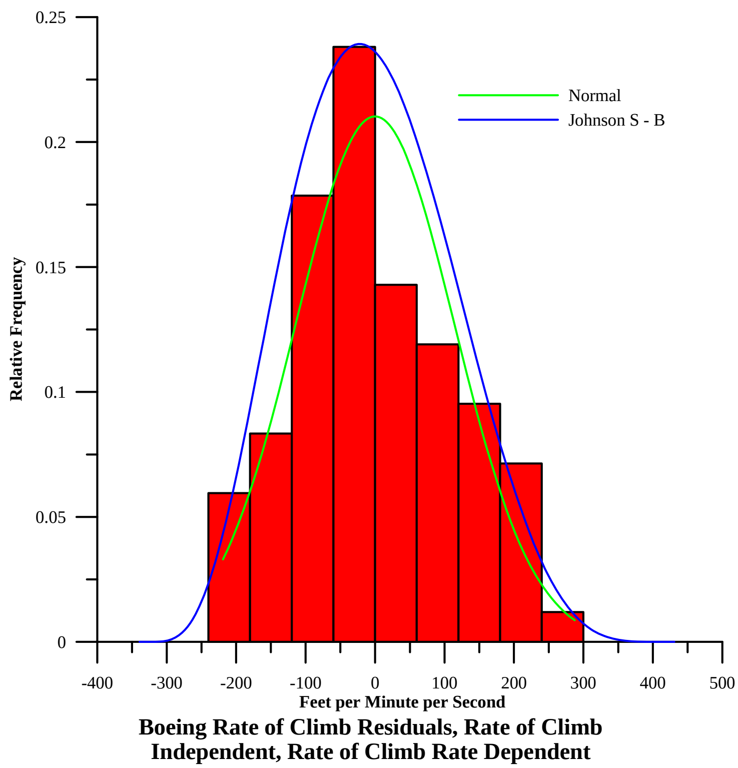

Figure 15: Johnson S – B Curve Fitted to Boeing Climb Residual Data

5.5 Comparison of Bank Angle Data by Aircraft Type

Tables 20, 21 and 22 display the comparative results for the bank angle data of the two aircraft. Table 21 indicates a significant difference in the dispersions, or standard deviations, of the two data sets. Table 22 indicates a significant difference in the means of the two data sets. Therefore, the two data sets cannot be combined into one set and two probability density functions are required. Figures 16 and 17 display histograms and probability density functions for the two data sets.

Table 21: Descriptive Statistics of Bank Angle by Aircraft Type

Descriptives of Bank Angle

Bank Angle [DEG]

	N	Mean	Std. Deviation	Std. Error	95% Confidence Interval for Mean		Minimum	Maximum
					Lower Bound	Upper Bound		
Airbus	74	24.22413	5.06824890	.58917197	23.0499094	25.3983455	16.90859	36.56289
Boeing	94	22.69244	4.03021495	.41568493	21.8669735	23.5179093	13.63729	36.03920
Total	168	23.36711	4.56677975	.35233471	22.6715084	24.0627168	13.63729	36.56289

Table 22: Levene's Test of Homogeneity of Variances of Bank Angle

Test of Homogeneity of Variances

Bank Angle [DEG]

Levene Statistic	df1	df2	Sig.
6.305	1	166	.013

Table 23: ANOVA of Bank Angle

ANOVA

Bank Angle [DEG]

	Sum of Squares	df	Mean Square	F	Sig.
Between Groups	97.138	1	97.138	4.763	.030
Within Groups	3385.727	166	20.396		
Total	3482.865	167			

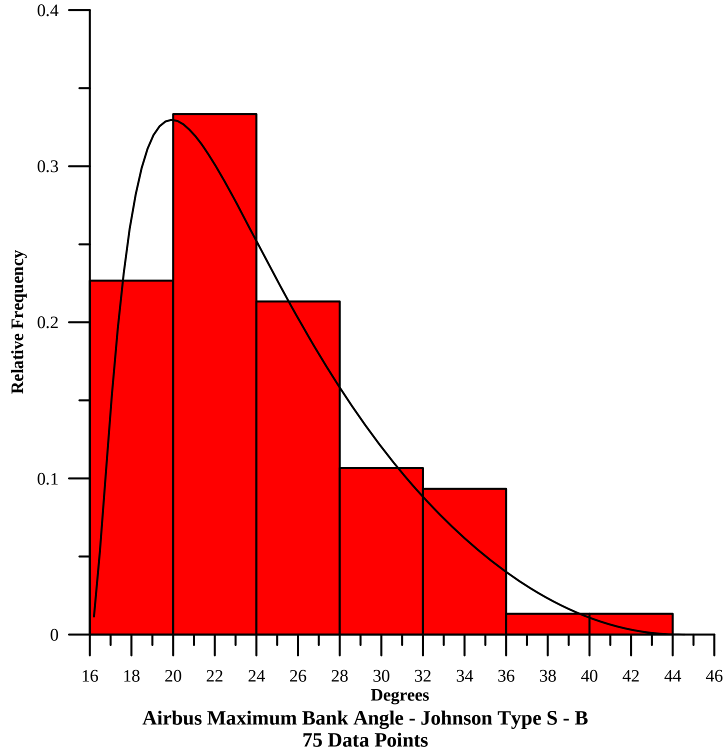

Figure 16: Airbus Maximum Bank Angle

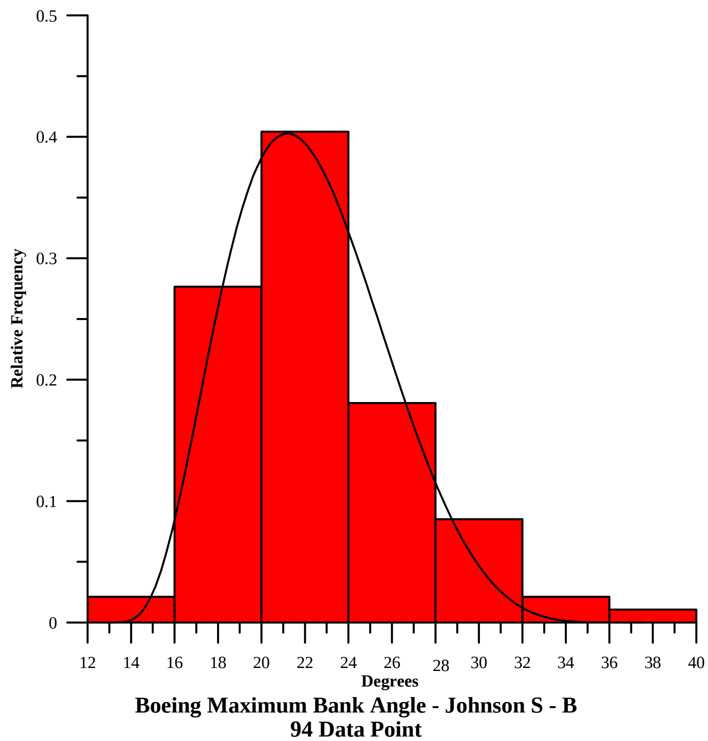

Figure 17: Boeing Maximum Bank Angle

5.6 Comparison of Roll Rate Data by Aircraft Type

Tables 24, 25 and 26 display the comparative results for the bank angle rate (roll rate) data of the two aircraft. Table 25 indicates no significant difference in the dispersions or standard deviations of the two data sets. Table 26 indicates a significant difference in the means of the two data sets. Therefore, the two data sets cannot be combined into one set and two probability density functions are required. Figures 18 and 19 display histograms and probability density functions for the two data sets.

Table 24: Descriptive Statistics of Bank Angle Rate by Aircraft Type

Descriptives Bank Angle Rate

Bank Rate [DEG/SEC]

					95% Confidence Interval for Mean			
	N	Mean	Std. Deviation	Std. Error	Lower Bound	Upper Bound	Minimum	Maximum
Airbus	74	3.79723	1.303503	.151529	3.49524	4.09923	1.386	6.608
Boeing	94	4.48326	1.890660	.195007	4.09601	4.87050	1.246	13.214
Total	168	4.18108	1.688211	.130248	3.92393	4.43822	1.246	13.214

Table 25: Levene's Test of Homogeneity of Variances of Bank Angle Rate

Test of Homogeneity of Variances

Bank Rate [DEG/SEC]

Levene Statistic	df1	df2	Sig.
3.039	1	166	.083

Table 26: ANOVA of Bank Angle Rate

ANOVA

Bank Rate [DEG/SEC]

	Sum of Squares	df	Mean Square	F	Sig.
Between Groups	19.486	1	19.486	7.086	.009
Within Groups	456.473	166	2.750		
Total	475.959	167			

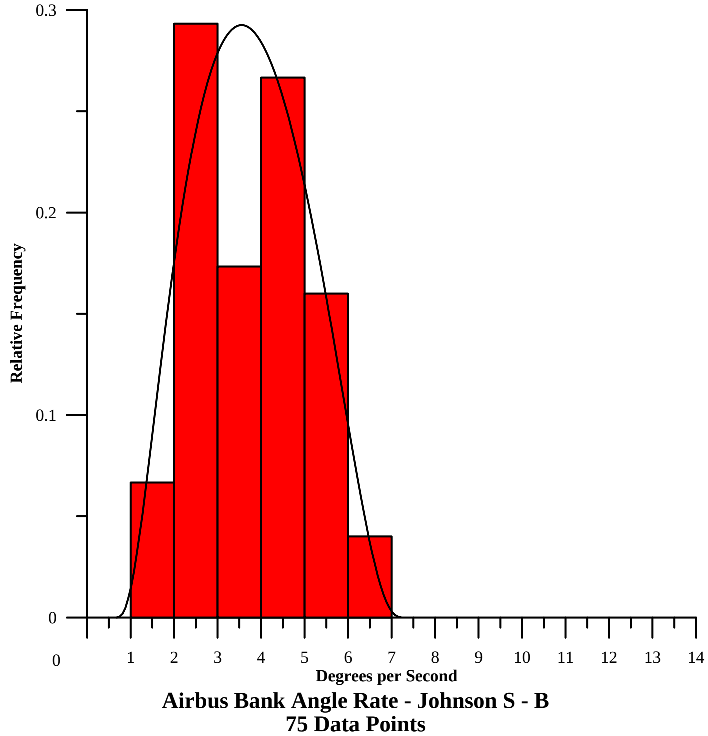

Figure 18: Airbus Bank Angle Rate

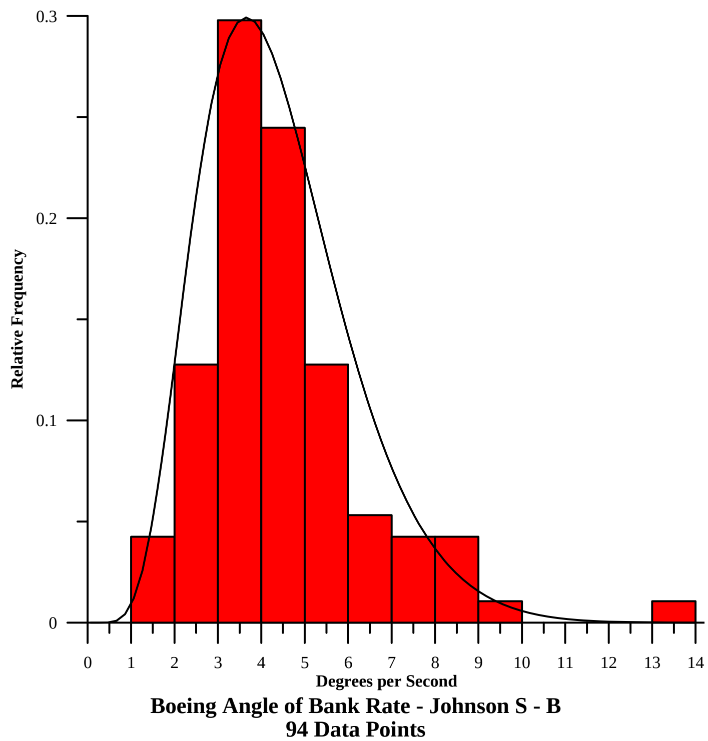

Figure 19: Boeing Bank Angle Rate

5.7 Correlation of Maximum Bank Angle with Bank Angle Rate

Tables 27 and 28 display the results of the Spearman rho test for the Airbus and Boeing maximum bank angle versus bank angle rate. The results indicate that there is a linear correlation for both aircraft data sets. Tables 29 and 30 display the results of the regression analysis. Figures 20 and 21 are scatter plots of the data for the Airbus and Boeing respectively.

Table 27: Spearman's rho Test of Airbus Correlation of Bank Rate versus Bank Angle

Airbus Correlations

			Bank Rate [DEG/SEC]	Bank Angle [DEG]
Spearman's rho	Bank Rate [DEG/SEC]	Correlation Coefficient	1.000	.602**
		Sig. (2-tailed)	.	.000
		N	74	74
	Bank Angle [DEG]	Correlation Coefficient	.602**	1.000
		Sig. (2-tailed)	.000	.
		N	74	74

**. Correlation is significant at the 0.01 level (2-tailed).

Table 28: Spearman's rho Test of Boeing Correlation of Bank Rate versus Bank Angle

Boeing Correlations

			Bank Angle [DEG]	Bank Rate [DEG/SEC]
Spearman's rho	Bank Angle [DEG]	Correlation Coefficient	1.000	.374**
		Sig. (2-tailed)	.	.000
		N	94	94
	Bank Rate [DEG/SEC]	Correlation Coefficient	.374**	1.000
		Sig. (2-tailed)	.000	.
		N	94	94

**. Correlation is significant at the 0.01 level (2-tailed).

Table 29: Airbus Regression Coefficients of Bank Angle versus Bank Rate

Airbus Coefficients Bank Angle Independent, Bank Rate Dependent[a]

Model		Unstandardized Coefficients		Standardized Coefficients	t	Sig.
		B	Std. Error	Beta		
1	(Constant)	.745	.591		1.260	.212
	Bank Angle [DEG]	.124	.024	.525	5.274	.000

a. Dependent Variable: Bank Rate [DEG/SEC]

Table 30: Boeing Regression Coefficients of Bank Angle versus Bank Rate

Boeing Coefficients Bank Angle Independent, Bank Rate Dependent[a]

Model		Unstandardized Coefficients		Standardized Coefficients	t	Sig.
		B	Std. Error	Beta		
1	(Constant)	.887	1.061		.836	.405
	Bank Angle [DEG]	.158	.046	.338	3.443	.001

a. Dependent Variable: Bank Rate [DEG/SEC]

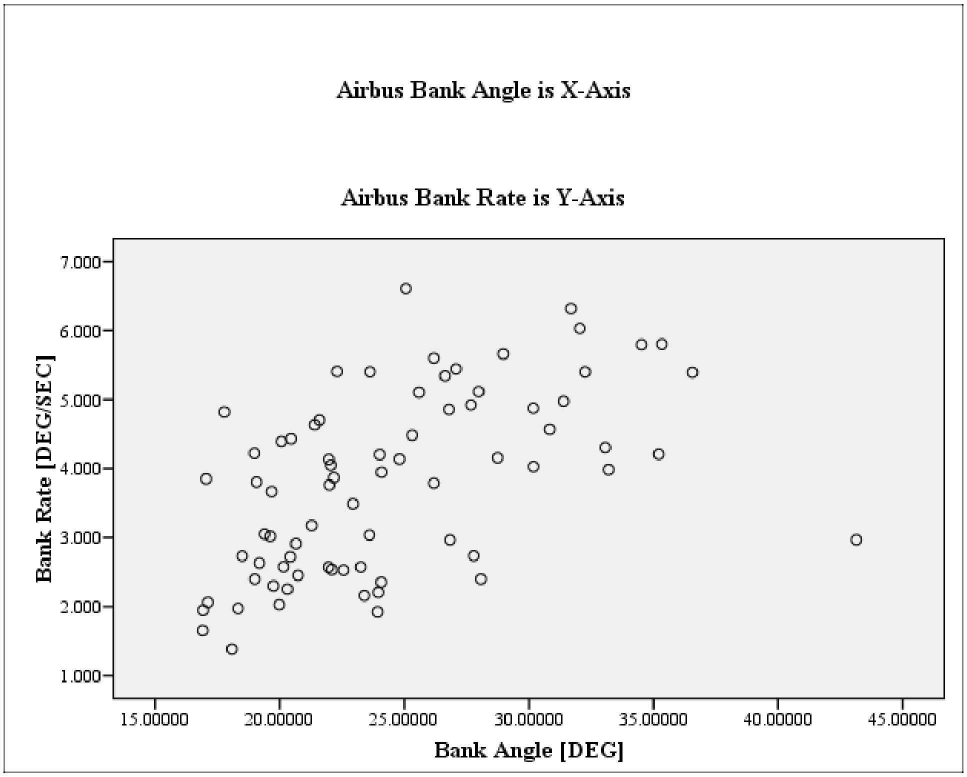

Figure 20: Airbus Scatter Plot of Bank Angle versus Bank Rate

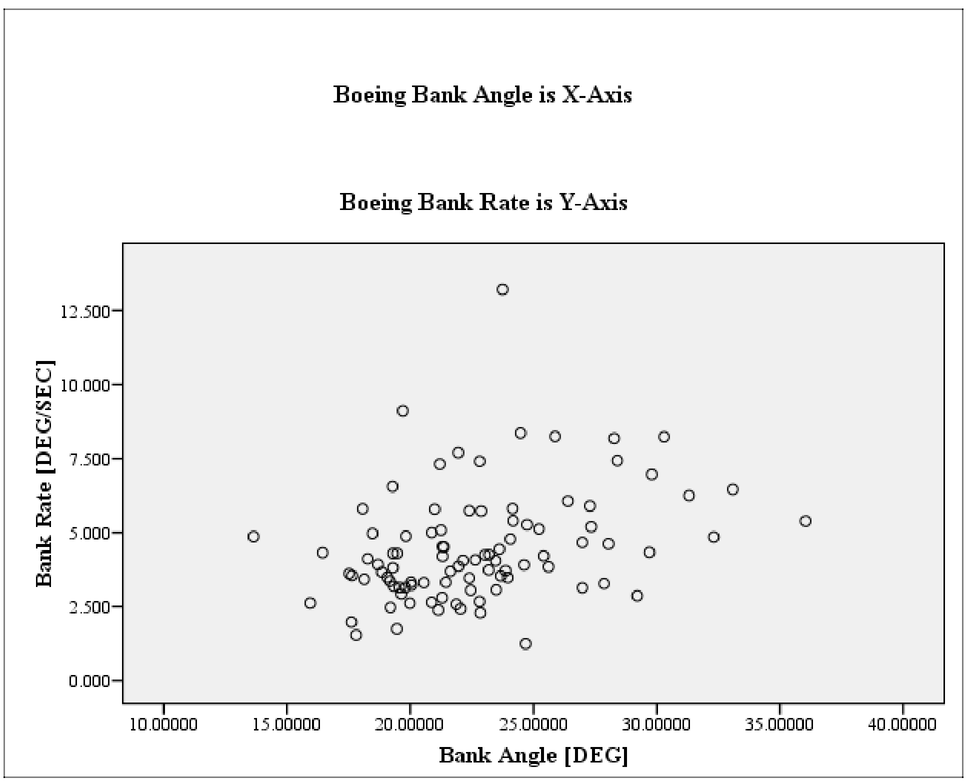

Figure 21: Boeing Scatter Plot of Bank Angle versus Bank Rate

5.8 Johnson Curves for the Sets of Bank Regression Residuals

Tables 31 and 32 display the results of two tests of normality, Kolmogorov-Smirnov and Shapiro-Wilk. In Table 31 the Kolmogorov-Smirnov test of Airbus residual data has a significance, or probability, of at least 0.200 and the Shapiro-Wilk test of Airbus residual data has a significance of 0.421. If either of these tests had produced a significance value less than 0.05, then the conclusion would have been that the data was not produced by a normal distribution. Therefore, the Airbus residual data can be modeled by a normal probability density function. The results of fitting a normal curve to the Airbus climb residual data are displayed in Figure 22. A Johnson S – B curve was also fitted to the data and is displayed in Figure 22. The Johnson curve follows closely the normal and has the advantage of being a bounded curve. Since a normal curve has infinite tails it is possible to draw very large or small unrealistic values while sampling in a Monte Carlo simulation. Since the Johnson curve is bounded, no unrealistic values can be drawn.

In Table 32 the Shapiro-Wilk test of Boeing residual data has a significance of 0.000. Therefore, the normality assumption for the Boeing residual data is rejected and the data must be modeled with a different pdf, such as a Johnson pdf. Figure 23 displays the result of fitting a Johnson S – B curve and a normal curve to the Boeing climb residual data.

Table 31: Airbus Tests of Normality of Bank Residuals

Airbus Tests of Normality of Bank Angle Residuals

	Kolmogorov-Smirnov[a]			Shapiro-Wilk		
	Statistic	df	Sig.	Statistic	df	Sig.
Unstandardized Residual	.077	75	.200*	.983	75	.421

*. This is a lower bound of the true significance.

a. Lilliefors Significance Correction

Table 32 Boeing Tests of Normality of Bank Residuals

Boeing Tests of Normality of Bank Angle Residuals

	Kolmogorov-Smirnov[a]			Shapiro-Wilk		
	Statistic	df	Sig.	Statistic	df	Sig.
Unstandardized Residual	.124	94	.001	.892	94	.000

a. Lilliefors Significance Correction

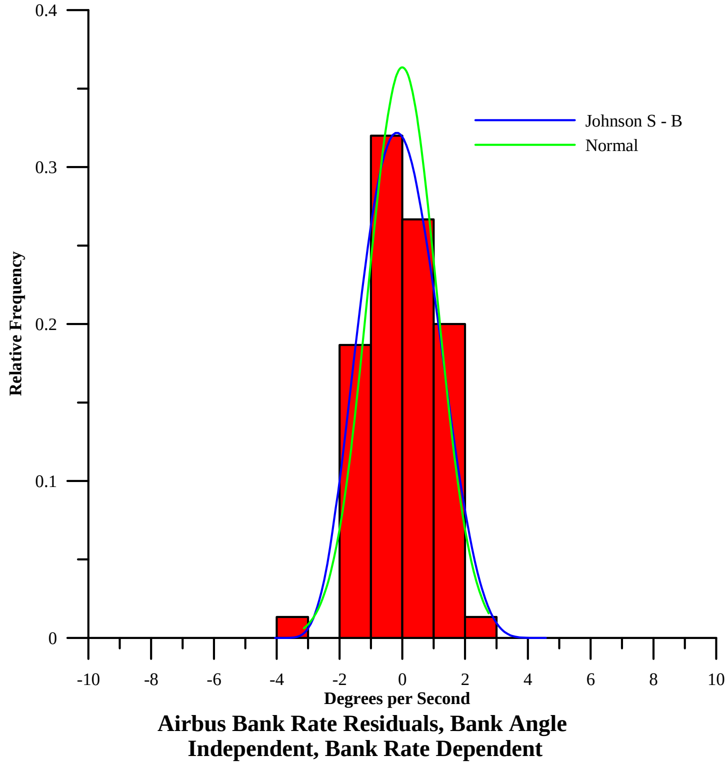

Figure 22: Normal Curve and Johnson S – B Curve Fitted to Airbus Bank Residual Data

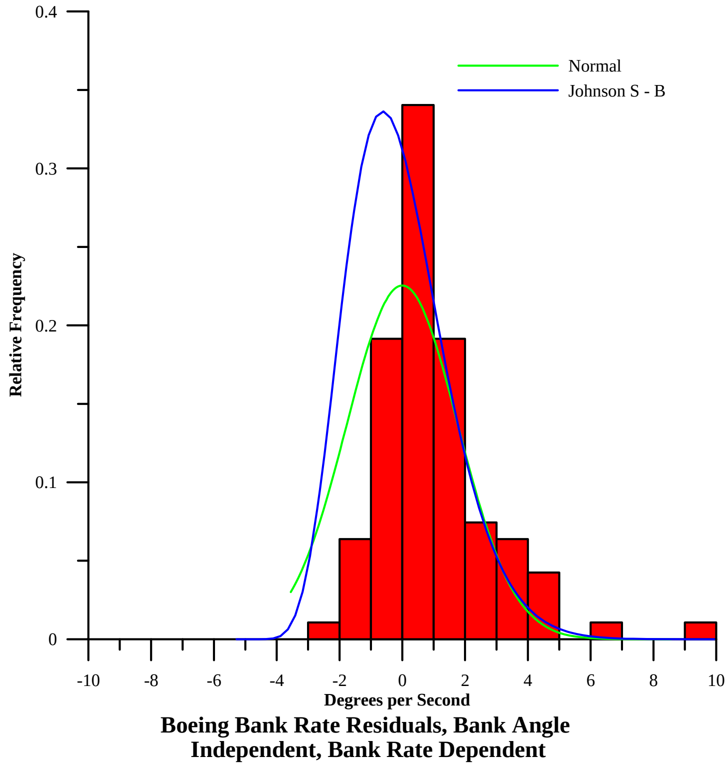

Figure 23: Johnson S – B Curve Fitted to Boeing Bank Residual Data

6.0 Airspace Simulation and Analysis Tool (ASAT)

The probability density functions described above will be incorporated into ASAT to perform fast-time, Monte Carlo simulations. The ASAT model is a new-generation Monte Carlo computer simulation system. It was developed to perform complex multiple aircraft simulations in the study of obstacle clearance and airspace requirements for new standards, the re-evaluation of existing standards and aircraft to aircraft collision risk assessment during approaches, departures, missed approaches, and operations within the terminal area.

7.0 Traffic Alert and Collision and Avoidance System (TCAS)

The TCAS Traffic Alerts were audibly annunciated and displayed continuously as a target offset and parallel to the crew. This was accepted by the pilots involved in the testing. Some crews actually attempted to use the displayed TA's to maintain their own separation from the target, or to monitor whether an adjacent aircraft was deviating from its course enough to cause a conflict. Resolution Advisories were inhibited in this DCE to avoid the issues experienced in the July 2009 DCE. TCAS could be a significant factor for avoiding accidents at any CSPO runway separation standard reduction

8.0 Conclusions and Recommendations

The principle measures of pilot response time are the time taken to begin the roll into the turn and the time taken to begin the throttle advance to initiate the climb. Since the two flight simulators involved in the data collection effort represented aircraft built by different manufacturers, the data was divided by aircraft type and tested for differences in response time means and dispersion.

8.1 Pilot Response Time to Roll from ATC Message

It was found that for the roll response data, the dispersions of the two data sets were not significantly different, but the mean response times were significantly different. Therefore probability density functions were determined for both sets of roll response data. The PRT mean for rolling the Airbus was determined to be 8.242 seconds with a standard deviation of 2.0294 seconds and for the Boeing the mean was 7.435 seconds with a standard deviation of 1.8607 seconds. (Note – PRT starts when the final controller depresses the PTT).

8.2 Pilot Response Time to Throttle from ATC Message

It was found that for the throttle response data, the dispersions of the two data sets were significantly different, but the mean response times were not significantly different. Therefore probability density functions were determined for both the sets of throttle response data. The PRT mean for throttle response for the Airbus was determined to be 9.061 seconds with a standard deviation of 3.2793 seconds and for the Boeing the mean was 8.965 seconds with a standard deviation of 2.4030 seconds.

8.3 Aircraft Dynamics

Since both roll and throttle responses are necessary to perform the breakout maneuver, the data were tested to determine whether roll and throttle responses were correlated. If correlation existed, it could indicate that a slow roll response was more likely to occur with a slow throttle response, or that one response was likely to precede the other. Tests of correlation showed no significant correlation.

The principle measures of aircraft performance derived from the test were maximum bank angle, roll rate, climb rate and acceleration into the climb. These data sets were also divided by aircraft manufacturer and tested for differences in dispersion and means.

It was found that the bank angle and roll rate data contained significant differences in either means or dispersion. These differences, and the probability density functions, had to be determined for each aircraft type and each data type.

The mean of the maximum bank angle for the Airbus was 24.221 degrees with a standard deviation of 5.068 degrees. The mean for the Boeing was 22.692 degrees with a standard deviation of 4.030 degrees.

The mean roll rate for the Airbus was 3.797 deg/sec with a standard deviation of 1.304 deg/sec. The mean for the Boeing was 4.483 deg/sec with a standard deviation of 1.891 deg/sec.
It was found that for the climb rate and acceleration into the climb data that significant differences existed in either means or dispersion and probability density functions had to the determined for each aircraft type and each data type.

The mean rate of climb for the Airbus was 2222.458 ft/min with a standard deviation of 655.571 ft/min, while the mean for the Boeing was 1975.688 ft/min with a standard deviation of 670.696 ft/min.

The mean rate of climb acceleration for the Airbus was 279.923 ft/min/sec with a standard deviation of 105.110 ft/min/sec, while the mean for the Boeing was 334.039 ft/min/sec with a standard deviation of 135.398 ft/min/sec.

It was found that the bank angle data and roll rate data were linearly coordinated and that the climb data and acceleration into the climb data were also linearly correlated. Correlation existed in both sets of the Airbus data and the Boeing data. Regression lines were determined and probability density functions were developed for both residual sets.

To obtain more realistic fast-time simulation results, it is recommended that the regression lines and residual probability density functions determined in this report be used in future simulations.

REFERENCES

[1] Project Plan CSPO-001: *Simultaneous Independent Dual Straight-In ILS Approaches with Runway Centerlines at 3,000 feet using a 4.8 second surveillance update rate*.

[2] Snedecor, George W; Cochran, William G; 1989; *Statistical Methods*, Blackwell Publishing; Ames, Iowa.

[3] Technical Report DOT-FAA-AFS-450-61. *Pilot and Controller Response Times from the JULY 2009 Human In The Loop Data Collection Project.*

APPENDIX A: Johnson Probability Density Function Parameters

Table A 1: Airbus Controller Message to Start of Roll Time

Johnson Type	S - B
Gamma	3.20503918
Delta	1.57208331
Lambda	26.2566068
Epsilon	4.59202512
Min	5.3
Max	15.3
data count	68.
ks probability	.59614

Table A 2: Airbus Controller Message to Start of Throttle Advance

Johnson Type	S - B
Gamma	2.317612834
Delta	1.353099477
Lambda	27.63602204
Epsilon	3.892129119
Min	4.8
Max	20.5
data count	65
ks probability	0.3512

Table A 3: Boeing Controller Message to Start of Roll Time

Johnson Type	S - B
Gamma	2.870119419
Delta	1.827379069
Lambda	21.44062067
Epsilon	3.32521077
Min	4.5
Max	14.6
data count	90
ks probability	0.75476

Table A 4: Boeing Controller Message to Start of Throttle Advance

Johnson Type	S - B
Gamma	2.447850184
Delta	1.707714706
Lambda	24.07271863
Epsilon	3.83056892
Min	5
Max	16.2
data count	93
ks probability	0.60107

Table A 5: Airbus Maximum Bank Angle

Johnson Type	S - B
Gamma	0.1100390766E+01
Delta	0.9962008935E+00
Lambda	0.2923000000E+02
Epsilon	0.1591000000E+02
Min	0.1691000000E+02
Max	0.4314000000E+02
data count	75
ks probability	0.79566

Table A 6: Airbus Bank Angle Rate

Johnson Type	S - B
Gamma	0.1799892279E+00
Delta	0.1140946422E+01
Lambda	0.6725733444E+01
Epsilon	0.6159486143E+00
Min	0.1390000000E+01
Max	0.6610000000E+01
data count	75
ks probability	0.36557

Table A 7: Airbus Rate of Climb

Johnson Type	S - B
Gamma	0.1965150263E+01
Delta	0.1868192807E+01
Lambda	0.1025628573E+04
Xi	-0.1783220774E+01
Min	0.1077300000E+03
Max	0.5780900000E+03
data count	59
ks probablility	0.37558

Table A 8: Airbus Rate of Climb Rate

Johnson Type	S - B
Gamma	-0.2561975974E-01
Delta	0.6924989924E+00
Lambda	0.2505110000E+04
Epsilon	0.9369000000E+03
Min	0.9379000000E+03
Max	0.3440010000E+04
data count	59
ks probability	0.65597

Table A 9: Boeing Maximum Bank Angle

Johnson Type	S - B
Gamma	0.8739970226E+00
Delta	0.1593570167E+01
Lambda	0.2540000000E+02
Xi	0.1264000000E+02
Min	0.1364000000E+02
Max	0.3604000000E+02
data count	94
ks probability	0.59530

Table A 10: Boeing Bank Angle Rate

Johnson Type	S - B
Gamma	0.8739970226E+00
Delta	0.1593570167E+01
Lambda	0.2540000000E+02
Xi	0.1264000000E+02
Min	0.1364000000E+02
Max	0.3604000000E+02
data count	94
ks probability	0.59530

Table A 11: Boeing Rate of Climb

Johnson Type	S - B
Gamma	0.5935442427E+00
Delta	0.1066806463E+01
Lambda	0.3099680000E+04
Xi	0.7639000000E+03
Min	0.7649000000E+03
Max	0.3861580000E+04
data count	84
ks probability	0.70029

Table A 12: Boeing Rate of Climb Rate

Johnson Type	S - B
Gamma	0.5248226461E+00
Delta	0.8957877712E+00
Lambda	0.6087923936E+03
Xi	0.9653230190E+02
Min	0.1215700000E+03
Max	0.6980400000E+03
data count	84
ks probability	0.56368

Table A 13: Airbus Bank Angle Residuals

Johnson Type	S - B
Gamma	0.3238837718E+00
Delta	0.1774715010E+01
Lambda	0.8885550000E+01
Xi	-0.4136340000E+01
Min	-0.3136340000E+01
Max	0.2749210000E+01
data count	75
ks probability	0.55659

Table A 14: Boeing Bank Angle Residuals

Johnson Type	S - B
Gamma	0.3281915723E+01
Delta	0.2590982511E+01
Lambda	0.2387679446E+02
Xi	-0.5517648614E+01
Min	-0.3552490000E+01
Max	0.8564580000E+01
data count	94
ks probability	0.55848

Table A 15: Airbus Climb Residuals

Johnson Type	S - B
Gamma	0.9672778333E+00
Delta	0.1438817081E+01
Lambda	0.6628038578E+03
Xi	-0.2374185911E+03
Min	-0.1587626800E+03
Max	0.2634495800E+03
data count	59
ks probability	0.72845

Table A 16: Boeing Climb Residuals

Johnson Type	S - B
Gamma	0.4656382648E+00
Delta	0.1582945207E+01
Lambda	0.7936686989E+03
Xi	-0.3470496526E+03
Min	-0.2190821300E+03
Max	0.2876101900E+03
data count	84
ks probability	0.58226

Table A 17: Regression Coefficients for Bank Angle Independent versus Bank Rate

	b_0	b_1
Airbus	0.745	0.124
Boeing	0.887	0.158

Table A 18: Regression Coefficients for Climb Rate Independent versus Climb Acceleration

	b_0	b_1
Airbus	151.110	0.058
Boeing	121.306	0.108